Macromolecules
ARTICLE

Macromolecules **2009**, *42*, 9183–9189 **9183**
DOI: 10.1021/ma901439u

Effects of Chain Topology on the Tracer Diffusion in Star Polyisoprenes

T. Cherdhirankorn,[†] G. Floudas,[‡] H.-J. Butt,[†] and K. Koynov*,[†]

[†]*Max-Planck-Institute for Polymer Research, D-55128 Mainz, Germany, and* [‡]*University of Ioannina, Department of Physics, P.O. Box 1186, 451 10 Ioannina, Greece and Foundation for Research and Technology-Hellas (FORTH), Biomedical Research Institute (BRI)*

Received July 3, 2009; Revised Manuscript Received October 19, 2009

ABSTRACT: Fluorescence correlation spectroscopy (FCS) was employed to study the effect of chain topology on the small tracer diffusion in linear and star-shaped 1,4-polyisoprenes (PIs) at temperatures well above the glass transition. In the linear polyisoprene, a Fickian diffusion behavior was observed that is characterized by a single diffusion coefficient. In contrast, the diffusion of the same tracers in three-arm star PI was non-Fickian and could best be described assuming two diffusion modes. The fast mode diffusion has the same magnitude and temperature dependence as the tracer diffusion in linear PI. The slow mode present only in the star polymer is apparently related to topological restrictions that cause retention of the tracer. The temperature dependence of the retention time is very similar to that of the polymer arm relaxation, indicating a direct correlation between the two dynamic processes.

Introduction

The diffusion of molecular tracers in polymers is of both fundamental and technological importance and thus has been intensely studied in the past two decades.[1−9] It was demonstrated that in contrast with the diffusion in simple liquids that is traditionally considered within the context of continuum hydrodynamics and described by the Stokes−Einstein equation (SE, $D \approx T/\eta$), the translational diffusion coefficients, D, of molecular tracers in polymer matrices scale with $\eta^{-\xi}$ with $\xi < 1$, where η is the polymer viscosity.[1,3,4,6] Furthermore, the tracer size, shape, and flexibility significantly affect the magnitude and temperature dependence of D.[3,4] To analyze the relation between the small tracers diffusion and the properties of the polymer matrix, free volume theories[1,10−13] and more recently atomistic molecular dynamics (MD) simulations[14−17] were applied. It is now broadly accepted that the diffusion of molecular tracers in a polymer matrix is coupled to the polymer segmental dynamics, that is, to the α-process associated with the glass transition. However, despite the extensive theoretical and experimental efforts,[2−4,6−9,18] the exact length scale involved in this coupling remains unclear. Practically all of the studies mentioned above were carried out with flexible linear polymers, and the effects of the polymer topology on the small tracer diffusion are not explored. For example, although the way that star-branched polymers diffuse into linear and star polymers has been investigated, we are not aware of any report on how small tracer molecules diffuse in star polymers.

The dynamic properties of branched polymers are different from those of linear polymers.[19−25] In an entangled melt of linear chains the relaxation time (reptation time), diffusion coefficient, and viscosity are given by

$$\begin{aligned} \tau &\approx \frac{\zeta_0 b^2}{k_B T}\frac{N^3}{N_e} \\ D &\approx \frac{k_B T}{\zeta_0}\frac{N_e}{N^2} \\ \eta &\approx \frac{\zeta_0 b^2}{v_0}\frac{N^3}{{N_e}^2} \end{aligned} \tag{1}$$

Here ζ_0, b, and v_0 are the monomer friction coefficient, length, and volume, respectively. N and N_e are the total number of monomers and the number of monomers in an entangled strand, respectively. In the case of entangled stars, the corresponding parameters are

$$\begin{aligned} \tau_{arm} &\approx \left(\frac{N_{arm}}{N_e}\right)^{5/2} \exp\left(\frac{N_{arm}}{N_e}\right) \\ D &\approx \left(\frac{N_{arm}}{N_e}\right)^{-5/2} \exp\left(-\frac{N_{arm}}{N_e}\right) \\ \eta &\approx \left(\frac{N_{arm}}{N_e}\right)^{3/2} \exp\left(\frac{N_{arm}}{N_e}\right) \end{aligned} \tag{2}$$

Here N_{arm} is the number of monomers per arm. Reptation is severely suppressed if the polymer has long arms. In this case, the center of the star can be considered to be fixed, and relaxation is only possible by contour length fluctuations, that is, by a process where the polymer retracts its arm down the tube and exits from the deformed tube.[26] This process gives rise to the exponential growth of the viscosity with the number of entanglements per arm, N_{arm}/N_e, and is predicted to be independent of the number of arms in the star.

Techniques utilized to study small tracer diffusion in bulk polymers include fluorescence recovery after photobleaching (FRAP),[2,27] fluorescence nonradiative energy transfer (NRET),[3,4] and forced Rayleigh scattering (FRS).[1,8,28] In recent years, fluorescence correlation spectroscopy (FCS) has emerged as a powerful tool for investigation of the diffusion of fluorescent molecules, macromolecules, or nanoparticles in various environments. FCS is based on detecting and analyzing the fluctuation of fluorescent light emitted by fluorescence species diffusing through a small ($< 1\ \mu m^3$) observation volume formed by a laser focused into the sample. Whereas it was initially developed and used mainly in biological environments, that is, aqueous solutions,[29] in the recent years, FCS was successfully applied to many classical polymer systems. In particular, the size and conformation of macromolecules in organic solvents,[30,31] adsorbed polymers,[32,33] cross-linked networks,[34,35] undiluted polymer solutions,[36−41] colloidal suspensions,[42] thin polymer films,[43] and bulk polymers[7,9] were studied.

*Corresponding author. E-mail: koynov@mpip-mainz.mpg.de.

Published on Web 10/30/2009

Table 1. Sources and Molecular Characteristics of the Polymer Samples

polymers	sample source	M_w (g/mol)	M_w/M_n	T_g (K)
LPI-22	in-house synthesis (MPIP)	22 500	1.06	208.4
SPI-10	PSS, Germany	10 150[a]	1.02	208.6
SPI-29	PSS, Germany	28 800[a]	1.02	208.1

[a] Arm molecular weight.

In this work, we explore, for the first time, the effect of chain topology on the diffusion of small molecular tracers in melts of linear and star-branched polyisoprenes (PIs). PI is a typical amorphous polymer, and its dynamic behavior was previously studied as a function of temperature[44,45] and pressure.[46,47] We employ FCS to determine the diffusion coefficients of terrylene dyes dispersed at nanomolar concentrations in matrices of linear and three-arm star polyisoprenes. We found distinctly different diffusional properties of the same tracer in the two topologies. Whereas in the linear polymer, a Fickian diffusion behavior was observed, in the three-arm star PI, the diffusion was anomalous and could best be described by two diffusion modes. We discuss the origin of the diffusion modes in relation to the polymer matrix dynamics.

Materials and Methods

Materials. Three-arm star polyisoprenes with arm molecular weights, M_{arm}, of 10 and 28.8 kg/mol were purchased from PSS, Mainz, Germany. In the text below, we refer to these materials as SPI-10 and SPI-29, respectively. Linear polyisoprene, LPI-22, with M_w of 22 kg/mol was prepared by living anionic polymerization. The molecular characteristics of all polymer samples are listed in Table 1. A terrylene dye, *N*,*N*′-bis(2,6-diisopropylphenyl)-1,6,9,14-tetraphenoxy-terrylene-3,4,11,12-tetracarboxidiimide (TDI), was selected as a molecular tracer because of its high quantum yield and good photostability.[48,49] The terrylene dye was first dissolved in tetrahydrofuran (THF) at a concentration of 10^{-5} M and then introduced into the host polymer. Pure solvent was added to aid the mixing, and the solution was mixed by a magnetic stirrer at a speed of 1000 rpm for 24 h. After mixing, the solvent was initially evaporated at 40 °C under vacuum for 3 to 4 h, and the sample was further annealed under vacuum at room temperature (25 °C) for 2 to 3 weeks. The final dye concentration in the polymer matrix (after solvent evaporation) was in the 10−100 nM range.

Fluorescence Correlation Spectroscopy. Measurements were carried out on a commercial FCS setup (Carl Zeiss, Jena, Germany) consisting of the module ConfoCor 2 and an inverted microscope model Axiovert 200. A 40× Plan Neofluar objective with a numerical aperture of 0.9 and oil as immersion liquid were used in this study. The terylene dye was excited by a HeNe laser at 633 nm, and the emission was collected after filtering with a LP650 long pass filter. For detection, an avalanche photodiode enabling single-photon counting was used. The average photon count rate was 30−40 kHz. An Attofluor steel cell (Invitrogen, Leiden, The Netherlands) with a microscope glass slide of 25 mm diameter and 0.15 mm thickness was used as a sample chamber. For each sample, a series of measurements of 60−90 min long were performed. The final results were obtained as an average of 3 to 4 experiments carried out on different days. For temperature control, a Linkam PE94 temperature control system (Linkam, Surrey, U.K.) was mounted on the microscope. A thermocouple wire was immersed in the sample to measure the actual temperature. During FCS measurements, the temperature, T, was kept constant ($\Delta T < 0.5$ °C). Our experimental setup allowed studies in the temperature range from 5 to 45 °C.

The time-dependent fluctuations of the fluorescence intensity, $\delta I(t)$, were recorded and analyzed by an autocorrelation function $G(t) = 1 + <\delta I(t')\,\delta I(t'+t)>/<I(t')>^2$. As has been shown theoretically for an ensemble of m different types of freely diffusing fluorescence species, $G(t)$ has the following analytical form[29]

$$G(t) = 1 + \left[1 + \frac{f_T}{1-f_T} e^{-t/\tau_T}\right] \frac{1}{N} \sum_{i=1}^{m} \frac{f_i}{\left[1 + \frac{t}{\tau_{D_i}}\right]\sqrt{1 + \frac{t}{S^2\tau_{D_i}}}} \quad (3)$$

Here N is the average number of diffusing fluorescence species in the observation volume, f_T and τ_T are the fraction and the decay time of the triplet state, τ_{D_i} is the diffusion time of the ith species, f_i is the fraction of component i, and S is the so-called structure parameter, $S = z_0/r_0$, where z_0 and r_0 represent the axial and radial dimensions of the confocal volume, respectively. Furthermore, the diffusion time, τ_{D_i}, is related to the respective diffusion coefficient, D_i, through[29]

$$\tau_{D_i} = \frac{r_0^2}{4D_i} \quad (4)$$

The experimentally obtained $G(t)$ can be fitted with eq 3 yielding the corresponding diffusion times; subsequently, the diffusion coefficients of the fluorescent species can be obtained from eq 4. However, because the value of r_0 depends strongly on the specific characteristics of the optical setup and the refractive index of the studied sample, a suitable calibration is required. In organic solvents or polymer melts, the calibrating procedure is not straightforward as in aqueous solution.[29] Recently, it was suggested that the calibration of the FCS observation volume in a given solvent can be made by independent measurements of the fluorescently labeled polymer diffusion coefficient by dynamic light scattering (DLS).[36−38,41] Here we applied a similar approach. The diffusion time of fluorescently labeled polystyrene ($M_w \approx 340$ kg/mol) dissolved in toluene was determined by FCS, and its diffusion coefficient (in the same solution) was measured by DLS. The value of r_0 was then determined by eq 4, yielding $r_0 = 0.32$ μm. Because toluene and polyisoprene have similar refractive indices ($n \approx 1.5$), the same value of r_0 was assumed for the PI studies.

Differential Scanning Calorimetry (DSC). Thermal characterization of polymers was performed using a Mettler DSC-30 calorimeter. Experiments were conducted with cooling and heating rates of 10 K/min. The glass-transition temperatures (T_g) were determined from the second heating run at the inflection point. All studied polymers (SPI-10, SPI-29, and LPI-22) showed similar values of T_g. (See Table 1).

Dynamic Mechanical Analysis (DMA). DMA has been performed using an ARES mechanical spectrometer (Rheometric Scientific). Shear deformation was applied under conditions of controlled deformation amplitude, which was kept in the range of the linear viscoelastic response of studied samples. A parallel plate geometry was used with plate diameters of 6 mm, and the gap between plates (sample thickness) was ∼1 mm. Experiments have been performed under a dry nitrogen atmosphere. Frequency dependencies of the storage (G') and the loss (G'') parts of the shear modulus have been determined from frequency sweeps measured within the frequency range of 10^{-2}−10^2 rad/s at various temperatures. Master curves for G' and G'' at a reference temperature, T_{ref}, have been obtained using the time−temperature superposition principle, $G^*(\omega,T) = G^*(a_T\omega,T_{ref})$, that is, by applying a single frequency-scale shift factor, a_T, at each temperature that allows superposition of all viscoelastic data at temperature, T, with the data at a reference temperature.

Dielectric Spectroscopy (DS). The sample cell consisted of two electrodes, 20 mm in diameter, and the sample with a thickness of 50 μm. The dielectric measurements were made at different temperatures in the range of 133.15−453.15 K under atmospheric pressure and for frequencies in the range from 3 × (10^{-3} to 10^6) Hz using a Novocontrol BDS system comprising a

frequency response analyzer (Solartron Schlumberger FRA 1260) and a broadband dielectric converter with an active sample head. The complex dielectric permittivity $\varepsilon^* = \varepsilon' - i\varepsilon''$, where ε' is the real part and ε'' is the imaginary part, is a function of frequency, f, temperature, T, and pressure, P, $\varepsilon^* = \varepsilon^*(\omega, T, P)$.[50] In the analysis, we used the empirical equation of Havriliak and Negami[51]

$$\varepsilon^*(T,P,\omega) = \varepsilon_\infty(T,P) + \frac{\Delta\varepsilon(T,P)}{[1+(i\omega\tau_{HN}(T,P))^{\alpha}]^{\gamma}} + \frac{\sigma_0(T,P)}{i\varepsilon_f\omega} \quad (5)$$

Here $\varepsilon_\infty(T,P)$ is the high-frequency permittivity, $\tau_{HN}(T,P)$ is the characteristic relaxation time in this equation, $\Delta\varepsilon(T,P) = \varepsilon_0(T,P) - \varepsilon_\infty(T,P)$ is the relaxation strength of the process investigated, α and γ (with limits $0 < \alpha$, $\alpha\gamma \leq 1$) describe, respectively, the symmetrical and asymmetrical broadening of the distribution of relaxation times, σ_0 is the dc conductivity, and ε_f is the vacuum permittivity. We have obtained master curves for the dielectric loss ε'' at a reference temperature by employing time−temperature superposition as $\varepsilon^*(f,T) = c_T\varepsilon^*(a'_T f, T_{ref})$, where c_T and a'_T are vertical and horizontal shift factors that allow superposition of all dielectric loss data taken at different temperatures with the data at the reference temperature.

Results and Dscussion

Figure 1a shows normalized autocorrelation curves $G(t)$ for TDI diffusing at room temperature in three-arm star polyisoprene (SPI-10) and in linear polyisoprene (LPI-22). The two materials are specially selected so that the molecular weight of the linear polymer is approximately equal to the span ($2M_{arm}$) molecular weight of the star PI. The autocorrelation curve measured in the linear polymer exhibits a single decay and can be fitted with eq 3 using one component only ($m = 1$). At the low fluorophore concentration used in the FCS experiments, the tracer mean-square displacement $<\Delta r^2(t)>$ can be obtained through[52]

$$G(t) = \frac{1}{N}\left(1+\frac{2}{3}\frac{\langle\Delta r^2(t)\rangle}{x_0^2}\right)^{-1}\left(1+\frac{2}{3}\frac{\langle\Delta r^2(t)\rangle}{z_0^2}\right)^{-1/2} \quad (6)$$

The inset in Figure 1 displays the mean square displacement $<\Delta r^2>$ versus time in a log−log plot. The data for the linear polyisoprene show a slope of 1, which indicates free Fickian diffusion of the TDI tracers. This finding reflects the spatial homogeneity of linear polyisoprene at temperatures well above T_g over the submicrometer length scale of the FCS experiment and is consistent with a number of other reports on small tracer diffusion in amorphous linear polymers.[3,8,9,28,53] In contrast, the log−log plot of the $<\Delta r^2>$ versus t for the TDI diffusing in the star polyisoprene (Figure 1, inset) exhibits a slope that depends on time, demonstrating noticeable deviation from Fickian behavior. Such anomalous tracer diffusion was observed in several amorphous linear polymers at temperatures close to T_g and was considered to be evidence of spatial heterogeneity of the polymer environment on a length scale on the order of 1 μm.[54,55] However, in the present work, all experiments were performed at temperatures well above the glass transition, and thus the possible reasons for the anomalous diffusion in the three-arm star PI should be traced to its different topology as compared with the linear PI. Indeed the presence of one additional branched chain at the middle of the span polymer molecules leads to heterogeneity in the three-arm star PI. The length scale of this heterogeneity (the distance between the centers of two neighboring star macromolecules), however, is on the order of a few nanometers, that

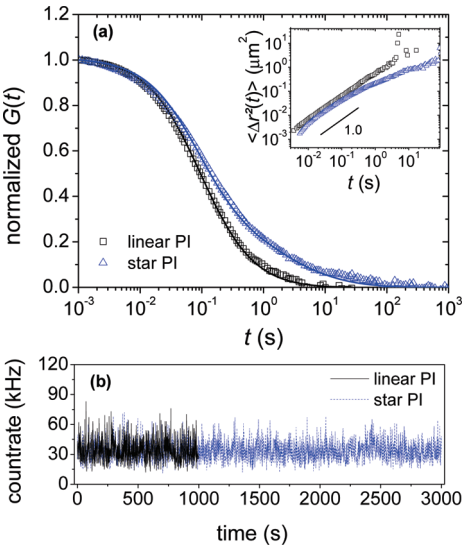

Figure 1. (a) Normalized autocorrelation curves for the diffusion of TDI in LPI-22 (M_w = 22 kg/mol) (□) and in SPI-10 (M_w = 3 × 10 kg/mol) (△). The solid lines represent the corresponding fits with eq 3 using $m = 1$ for LPI-22 and $m = 2$ for SPI-10. The inset presents the dependence of the mean-square displacement on time. (b) Corresponding time traces.

means, much smaller than the FCS sampling volume (~1 μm^3), and therefore cannot be a direct reason for the observed anomalous diffusion behavior.

To get better insight into this issue, we have attempted to fit the autocorrelation curve measured for the TDI diffusing in the star polyisoprene (Figure 1a). Two different approaches have been commonly used to fit FCS autocorrelation curves in the case of anomalous diffusion. The first one is based on the assumption that the mean squared displacement is no longer directly proportional to time but rather depends on t^α yielding[56−60]

$$G(t) = 1 + \left[1+\frac{f_T}{1-f_T}e^{-t/\tau_T}\right]\frac{1}{N}\frac{1}{\left[1+\left(\frac{t}{\tau_{anom}}\right)^{\alpha}\right]\sqrt{1+\frac{1}{S^2}\left(\frac{t}{\tau_{anom}}\right)^{\alpha}}} \quad (7)$$

The second approach is to use a multicomponent fit, for example, to apply eq 3 with $m = 2$. The latter approach assumes temporal trapping of the diffusing fluorescent tracers in immobile sites within the FCS observation volume that give rise to an additional slower diffusion component.[61−63] A number of more complicated expressions for the autocorrelation function in the case of anomalous diffusion were also recently suggested.[63−65]

Applying eq 7 to our experimental data for TDI diffusing in the SPI-10 did not produce a reasonable fit. In contrast, using eq 3 with two diffusing components ($m = 2$) allowed a very good fit of the experimental data (Figure 1a). In general, the two diffusing components may reflect the presence of two different types of fluorescent tracers. This possibility, however, can be excluded for the following reasons. All studied polymer samples were carefully examined before the addition of the TDI tracers and did not show any autofluorescence at the used excitation/emission wavelengths. This means that the only fluorescent species in the studied systems were single TDI molecules and eventually aggregates of such molecules, for example, dimers, trimers, and so on. However, aggregation is unlikely at the nanomolar TDI concentration used in this study; moreover, in all experiments, the observed number of fluorescent tracers in the observation volume was very close to the estimation based on the TDI concentration used for sample preparation. Furthermore, there is no reason

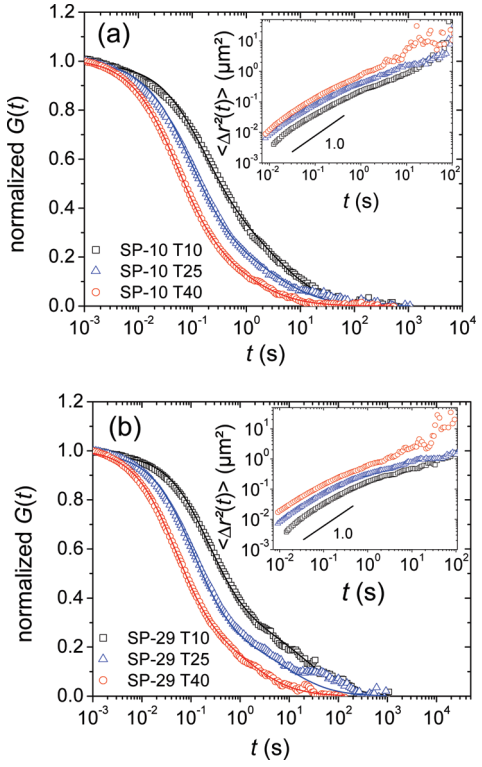

Figure 2. Experimental autocorrelation curves (symbols) and the corresponding fits with eq 3 using $m = 2$ (solid lines) for TDI diffusion in (a) SPI-10 and (b) SPI-29 at different temperatures: □, 10 °C; △, 25 °C; and ○, 40 °C. The insets give the dependence of the mean-square displacement on time. Slopes of 1 are shown for comparison.

why aggregates should be present only in the three-arm star PI and not in the linear PI melts, especially taking into account the fact that the measured molecular brightness of the fluorescent tracers was practically the same in both PI topologies. Finally, even if one assumes the presence of dimers or trimers in the star PI only, their diffusion coefficients should be rather similar to that of the single molecules and not two orders of magnitude smaller (see below), as we have found. Another possible reason for the appearance of slow component in the autocorrelation curves may be the eventual photobleaching of the fluorescent tracers. However the TDI tracers have an extremely good photostability and have shown no bleaching over the extended periods of data acquisition used for the studies of three-arm star PI. This is illustrated in Figure 1b, which shows a typical time trace, that is, the time dependence of the measured fluorescent intensity, $I(t')$, during an FCS experiment. As can be seen, there is no decrease in the count rate, even after 3000 s.

The two-component fit, therefore, indicates that although only one type of fluorescence species exists (single TDI molecules), they diffuse with two distinct rates in the star polymers. Similar bimodal diffusion was also observed in the star polyisoprenes at higher temperatures. Figure 2a,b presents the normalized autocorrelation curves of TDI diffusion at different temperatures in SPI-10 and SPI-29, respectively.

All autocorrelation curves reveal two distinct diffusion times and can be nicely described with eq 3 using two components ($m = 2$). The mean-square displacements, $<\Delta r^2>$ versus t in a log−log plot, are again not merely proportional, but the slope depends on time (Figure 2, insets).

By fitting the experimental autocorrelation curves obtained for TDI diffusion in the star polymers with eq 1, two distinct diffusion times were obtained, τ_1 and τ_2, representing the "fast" and the "slow" modes, respectively. Furthermore, the fractions

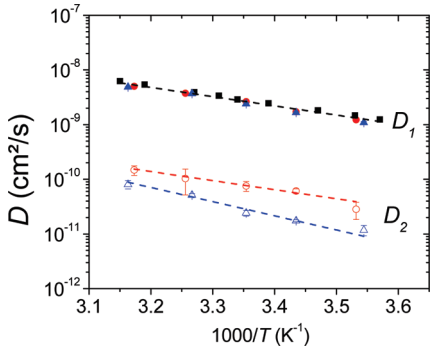

Figure 3. Diffusion coefficients calculated from τ_1 for TDI in linear LPI-22 (■), SPI-10 (●), and SPI-29 (▲). Apparent diffusion coefficient calculated from τ_2 for TDI in SPI-10 (○) and SPI-29 (△). Dashed lines represent the result of a fit to an Arrhenius equation.

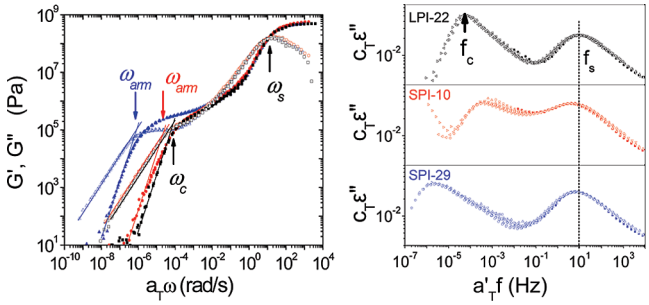

Figure 4. Left: Master curves of the storage modulus (G') and loss modulus (G'') of LPI-22 (■,□), SPI-10 (●,○), and SPI-29 (▲,△) constructed at a reference temperature of 215 K. The arrows show the radial frequencies corresponding to the segmental (ω_S), terminal (ω_c), and arm relaxation in the stars (ω_{arm}). Right: Master curves of the dielectric loss (ε'') of LPI-22 (top), the SPI-10 (middle), and the SPI-29 (bottom) at a reference temperature of 218 K. The different symbols correspond to temperatures in the range from 218−258, 218−248, and 218−243 K for the LPI-22, SPI-10, and SPI-29, respectively. The vertical line signifies the characteristic frequency for the segmental process, whereas the arrow, indicated as f_c, depicts the characteristic frequency of the chain (terminal) relaxation in LPI-22 at the reference temperature.

of these two components (f_i in eq 1) are found to be $f_1 \approx 70\%$ and $f_2 \approx 30\%$.

From the diffusion times, τ_1 and τ_2, the corresponding diffusion coefficients, D_1 and D_2, can be calculated using eq 4. The temperature dependence of D_1 and D_2 for TDI diffusing in SPI-10 and SPI-29 are shown in Figure 3. For comparison, the temperature dependence of the diffusion coefficient of TDI in LPI-22 is also plotted. At all temperatures, the value of the "fast" mode diffusion coefficients, D_1, in both star polyisoprenes is practically the same as the TDI diffusion coefficient in the linear polymer. This indicates that the fast diffusion mode observed in the star PI originates from the same physical effects as the diffusion in linear PI.

As previously discussed,[2−4,6−9,18] the tracer diffusion in linear polymers is correlated to the polymer segmental dynamics. Such correlation will impose that our diffusion studies indicate similar segmental dynamics in the linear and the star polyisoprenes. To explore this issue further, we have studied the segmental relaxation dynamics of LPI-22, SPI-10, and SPI-29 using rheology and dielectric spectroscopy. The mechanical spectra of LPI-22 and the two star polymers display two major relaxation processes (Figure 4). The high-frequency mode corresponds to the segmental relaxation ($\tau_s = 2\pi/\omega_s$). The mode at lower frequencies corresponds to the chain (terminal) relaxation ($\tau_c = 2\pi/\omega_c$) in the linear PI and to the arm relaxation ($\tau_{arm} = 2\pi/\omega_{arm}$) in the stars.

We should mention here that relating the low-frequency mode to the arm relaxation is exact only in SPI-29. The low-molecular-weight star SPI-10 is barely, if at all, entangled (PI entanglement molecular weight $M_e \approx 6400$ g/mol),[66] and this relation is only an approximation. In the same Figure, the corresponding dielectric loss spectra for the three polymers are compared at a reference temperature of 218 K. In the LPI-22, the two main processes correspond to the segmental (f_s) and chain or terminal processes (f_c). Notice the breakdown of time−temperature superposition that is more apparent in DS because of the broader frequency range available.[45,47]

Independent of the method, the segmental relaxations in linear and star PI occur at similar frequencies at the corresponding reference temperature. This is illustrated in Figure 5, where the temperature dependence of τ_s evaluated from DMA and DS is shown. The identical segmental dynamics in both topologies of PI, combined with the identical TDI diffusion coefficient in linear PI and the fast diffusion mode in star PI (Figure 3), constitutes further evidence of the tracer diffusion being correlated to the polymer segmental relaxation. The exact connection, however, still remains unknown because of the length scale involved.

As discussed above, in contrast with the single decay of the autocorrelation curve from tracer diffusion in linear PI, an additional mode with a long time scale arises in the star PIs. The major difference of the star polymers as compared with the linear one is the additional branched point in the star center. Furthermore, the dynamics of a star polymer with long (entangled) arms, is different from that of a linear polymer (eqs 1 and 2). In a star polymer composed of f arms, reptation is suppressed because the molecule would have to drag f-1 arms along the tube of a single arm. Instead, the center of the star is localized within a distance corresponding to the tube diameter, and the star can relax only by arm retraction (eq 2).

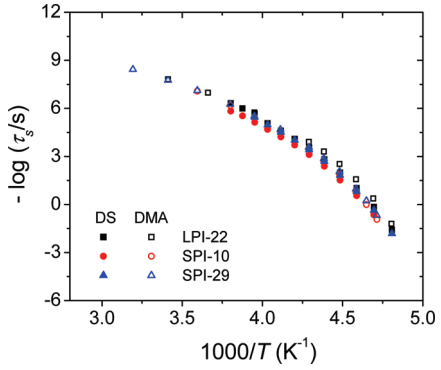

Figure 5. Segmental relaxation times of star and linear PI as measured by dynamic mechanical analysis (DMA) and dielectric spectroscopy (DS) plotted in the usual Arrhenius representation.

In an FCS study, the observation length-scale is much larger than any molecular scale. It is reasonable to assume, therefore, that the star polymer does not diffuse through the FCS observation volume on the time scale of the FCS measurement. With this assumption in mind, the bimodal distribution for a molecular probe in the star PI can be understood as follows. Most tracer molecules (>70%) can diffuse through the FCS observation volume (<1 μm^3) without any special restriction arising from the star topology. These tracers give rise to the fast mode diffusion, which is basically the same as that in the linear polymer. Some tracers however, can be physically trapped in a certain point of the polymer matrix and stay at this state (or diffuse extremely slowly) for a certain time. Eventually, such tracers are released and then join the normal fast diffusion channel. This trapping−releasing process, which is not observed in linear PI, should be related to the special topology of the three-arm stars, that is, the existence of a branched point in the star center that can only relax through the arm retraction process.

Such a physical picture imposes that the characteristic time of the slow mode should be considered as a combination of a retention time and a fast diffusion time. Because the slow time, τ_2, is about two decades longer than the diffusion time, τ_1, the contribution of fast diffusion is negligible and τ_2 is approximately equal to the retention time. The likelihood for a tracer to be trapped in the observation volume is low, and thus most tracers diffuse freely through the observation volume, as confirmed by the high fraction ($f_1 \approx 70\%$) of the fast process.

At this point, it is natural to explore the relation between the retention time observed in the three-arm stars and the corresponding arm relaxation. The latter can be extracted from the slowest mode in rheology (arm relaxation). Its temperature dependence is depicted in an Arrhenius representation in Figure 6.

The $\tau_{arm}(T)$ conforms to the Vogel−Fulcher−Tammann (VFT) equation

$$\tau_{arm} = \tau_0 \exp\left(\frac{B}{T - T_0}\right) \quad (8)$$

Here τ_0 is the characteristic time at high temperatures, B is the activation parameter, and T_0 is the freezing temperature. The temperature dependence of the retention time, τ_2, obtained from FCS for both star polymers is directly compared with $\tau_{arm}(T)$ obtained from rheology. From Figure 6a,b, it is seen that the retention time is around two orders of magnitude slower than the arm relaxation time. However, whereas both processes are different in magnitude, they exhibit similar temperature dependences (Figure 6). In addition, the ratio of the retention times for

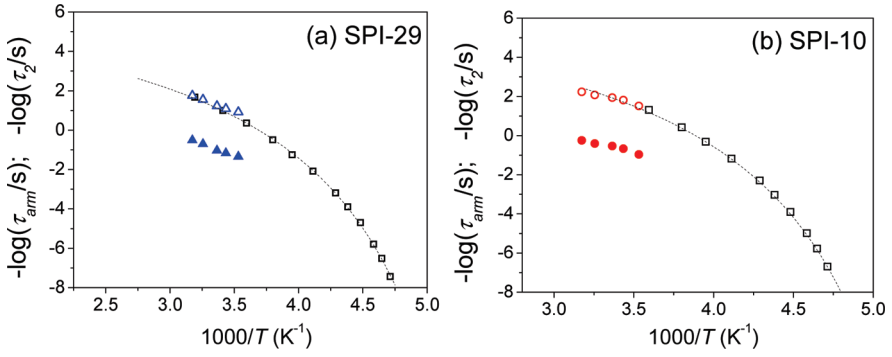

Figure 6. (a) Temperature dependence of the retention times corresponding to the FCS "slow" mode, τ_2 (▲), and of the arm relaxation (obtained from rheology), τ_{arm} (□), for the SPI-29; τ_2 shifted by a factor 2.3 (△) is also shown for comparison. (b) Temperature dependence of the retention times corresponding to the FCS "slow" mode, τ_2 (●), and of the arm relaxation (obtained from rheology), τ_{arm} (□), for the SPI-10; τ_2 shifted by a factor of 2.5 (○) is also shown for comparison. Lines are fits to the VFT equation.

the TDI diffusing in the stars, that is, $\tau_2^{\text{SPI-10}}/\tau_2^{\text{SPI-29}} \approx 0.03$, is similar to the ratio of $\tau_{\text{arm}}^{\text{SPI-10}}/\tau_{\text{arm}}^{\text{SPI-29}}$ corresponding to the arm relaxation process in rheology. Therefore, the temperature and molecular weight dependencies suggest that the slow mode in FCS follows the arm retraction in the star polymer.

Conclusions

We used FCS to explore the effect of chain topology on the small tracer diffusion in linear and star-shaped PI at temperatures well above the glass transition. The unique, single molecule sensitivity of the FCS technique allows us to perform studies at nanomolar tracer concentrations, ensuring that the tracers do not modify the matrix polymer properties. In the linear polyisoprene, a Fickian diffusion of TDI molecules was observed, characterized by a single diffusion coefficient. This finding reflects the spatial homogeneity of the linear polyisoprene at temperatures well above T_g on the submicrometer length scales of the FCS experiments and is consistent with a number of previous reports on small tracer diffusion in amorphous linear polymers. In contrast, the diffusion of the same TDI tracers in three-arm star PI was non-Fickian on the length scale of the probing volume ($< 1\ \mu m^3$), and the corresponding FCS autocorrelation curves can best be described by assuming two distinct time constants. The fast mode corresponds to a tracer diffusion coefficient that has the same magnitude and temperature dependence as the tracer diffusion coefficient in linear PI. This finding can be considered to be further evidence of the tracer diffusion being linked to the segmental dynamics of the host polymer, which is identical in the star and linear PI. The slow mode, which was found only in the star polymers, is related to topological restrictions that may cause retention of the tracer. The temperature and molecular weight dependence of the retention time were very similar to those of the arm relaxation in the stars, suggesting a common origin.

Acknowledgment. We thank George Fytas and Vagelis Harmandaris for the helpful discussions, Klaus Müllen and Kalina Peneva for the synthesis of TDI, and A. Best, A. Hanewald, T. Wagner, and J. Thiel for the technical assistance. T.C. acknowledges a Marie Curie fellowship for early stage research training (EST) for the financial support.

References and Notes

(1) Ehlich, D.; Sillescu, H. *Macromolecules* **1990**, *23*, 1600–1610.
(2) Cicerone, M. T.; Blackburn, F. R.; Ediger, M. D. *Macromolecules* **1995**, *28*, 8224–8232.
(3) Deppe, D. D.; Miller, R. D.; Torkelson, J. M. *J. Polym. Sci., Part B: Polym. Phys.* **1996**, *34*, 2987–2997.
(4) Hall, D. B.; Deppe, D. D.; Hamilton, K. E.; Dhinojwala, A.; Torkelson, J. M. *J. Non-Cryst. Solids* **1998**, *235*−*237*, 48–56.
(5) Tseng, K. C.; Turro, N. J.; Durning, C. J. *Polymer* **2000**, *41*, 4751–4755.
(6) Ediger, M. D. *Annu. Rev. Phys. Chem.* **2000**, *51*, 99–128.
(7) Best, A.; Pakula, T.; Fytas, G. *Macromolecules* **2005**, *38*, 4539–41.
(8) Maji, S.; Urakawa, O.; Adachi, K. *Polymer* **2007**, *48*, 1343–1351.
(9) Cherdhirankorn, T.; Harmandaris, V.; Juhari, A.; Voudouris, P.; Fytas, G.; Kremer, K.; Koynov, K. *Macromolecules* **2009**, *42*, 4858–4866.
(10) Bueche, F. *Physical Properties of Polymers*; Interscience: New York, 1962.
(11) Vrentas, J. S.; Duda, J. L. *J. Appl. Polym. Sci.* **1978**, *22*, 2325–2339.
(12) Vrentas, J. S.; Vrentas, C. M. *Macromolecules* **1993**, *26*, 1277–1281.
(13) von Meerwall, E.; Feick, E. J.; Ozisik, R.; Mattice, W. L. *J. Chem. Phys.* **1999**, *111*, 750–757.
(14) Gusev, A. A.; Suter, U. W. *J. Chem. Phys.* **1993**, *99*, 2228–2234.
(15) Harmandaris, V. A.; Angelopoulou, D.; Mavrantzas, V. G.; Theodorou, D. N. *J. Chem. Phys.* **2002**, *116*, 7656–7665.
(16) Muller-Plathe, F.; Rogers, S. C.; Vangunsteren, W. F. *Chem. Phys. Lett.* **1992**, *199*, 237–243.
(17) Theodorou, D. N. Molecular Simulations of Sorption and Diffusion in Amorphous Polymers. In *Diffusion in Polymers*; Neogi, P., Ed.; Marcel Dekker: New York, 1996.
(18) Adachi, K. *Macromolecules* **1990**, *23*, 1816–1821.
(19) Carella, J. M.; Gotro, J. T.; Graessley, W. W. *Macromolecules* **1986**, *19*, 659–667.
(20) Boese, D.; Kremer, F.; Fetters, L. J. *Macromolecules* **1990**, *23*, 1826–1830.
(21) Fetters, L. J.; Kiss, A. D.; Pearson, D. S.; Quack, G. F.; Vitus, F. J. *Macromolecules* **1993**, *26*, 647–654.
(22) Bero, C. A.; Roland, C. M. *Macromolecules* **1996**, *29*, 1562–1568.
(23) Roland, C. M.; Bero, C. A. *Macromolecules* **1996**, *29*, 7521–7526.
(24) Ngai, K. L.; Roland, C. M. *J. Polym. Sci., Part B: Polym. Phys.* **1997**, *35*, 2503–2510.
(25) Watanabe, H.; Matsumiya, Y.; Inoue, T. *Macromolecules* **2002**, *35*, 2339–2357.
(26) Doi, M.; Edwards, S. F. *The Theory of Polymer Dynamics*; Clarendon Press: Oxford, U.K., 1986.
(27) Rajian, J. R.; Quitevis, E. L. *J. Chem. Phys.* **2007**, *126*, 224506−1–10.
(28) Veniaminov, A. V.; Sillescu, H. *Macromolecules* **1999**, *32*, 1828–1837.
(29) Rigler, R.; Elson, E. S. *Fluorescence Correlation Spectroscopy*; Springer-Verlag: New York, 2001.
(30) Kim, B. S.; Lebedeva, O. V.; Koynov, K.; Gong, H.; Glasser, G.; Lieberwith, I.; Vinogradova, O. I. *Macromolecules* **2005**, *38*, 5214–5222.
(31) Koynov, K.; Mihov, G.; Mondeshki, M.; Moon, C.; Spiess, H. W.; Müllen, K.; Butt, H.-J.; Floudas, G. *Biomacromolecules* **2007**, *8*, 1745–1750.
(32) Sukhishvili, S. A.; Chen, Y.; Müller, J. D.; Gratton, E.; Schweizer, K. S.; Granick, S. *Macromolecules* **2002**, *35*, 1776–1784.
(33) Zhao, J.; Granick, S. *Macromolecules* **2007**, *40*, 1243–1247.
(34) Gianneli, M.; Beines, P. W.; Roskamp, R. F.; Koynov, K.; Fytas, G.; Knoll, W. *J. Phys. Chem. C* **2007**, *111*, 13205–13211.
(35) Zhang, R.; Cherdhirankorn, T.; Graf, K.; Koynov, K.; Berger, R. *Microelectron. Eng.* **2008**, *85*, 1261–1264.
(36) Zettl, H.; Häfner, W.; Böker, A.; Schmalz, H.; Lanzendörfer, M.; Müller, A. H. E.; Krausch, G. *Macromolecules* **2004**, *37*, 1917–1920.
(37) Liu, R.; Gao, X.; Adams, J.; Oppermann, W. *Macromolecules* **2005**, *38*, 8845–8849.
(38) Zettl, H.; Zettl, U.; Krausch, G. *Phys. Rev. E* **2007**, *75*, 061804.
(39) Grabowski, C. A.; Mukhopadhyay, A. *Macromolecules* **2008**, *41*, 6191–6194.
(40) Wöll, D.; Uji-i, H.; Schnitzler, T.; Hotta, J. I.; Dedecker, P.; Herrmann, A.; De Schryver, F. C.; Müllen, K.; Hofkens, J. *Angew. Chem., Int. Ed.* **2008**, *47*, 783–787.
(41) Cherdhirankorn, T.; Best, A.; Koynov, K.; Peneva, K.; Müllen, K.; Fytas, G. *J. Phys. Chem. B* **2009**, *113*, 3355–3359.
(42) Kang, K.; Gapinski, J.; Lettinga, M. P.; Buitenhuis, J.; Meier, G.; Ratajczyk, M.; Dhont, J. K. G.; Patkowski, A. *J. Chem. Phys.* **2005**, *122*, 044905.
(43) Casoli, A.; Schönhoff, M. *Biol. Chem.* **2001**, *382*, 363–369.
(44) Adachi, K.; Kotaka, T. *Macromolecules* **1985**, *18*, 466–472.
(45) Plazek, D. J.; Schlosser, E.; Schonhals, A.; Ngai, K. L. *J. Chem. Phys.* **1993**, *98*, 6488–6491.
(46) Floudas, G.; Gravalides, C.; Reisinger, T.; Wegner, G. *J. Chem. Phys.* **1999**, *111*, 9847–9852.
(47) Floudas, G.; Reisinger, T. *J. Chem. Phys.* **1999**, *111*, 5201–5204.
(48) Nolde, F.; Qu, J. Q.; Kohl, C.; Pschirer, N. G.; Reuther, E.; Mullen, K. *Chem.—Eur. J.* **2005**, *11*, 3959–3967.
(49) Jung, C.; Müller, B. K.; Lamb, D. C.; Nolde, F.; Müllen, K.; Bräuchle, C. *J. Am. Chem. Soc.* **2006**, *128*, 5283–5291.
(50) Floudas, G. *Prog. Polym. Sci.* **2004**, *29*, 1143–1171.
(51) Havriliak, S.; Negami, S. *Polymer* **1967**, *8*, 161.
(52) Shusterman, R.; Alon, S.; Gavrinyov, T.; Krichevsky, O. *Phys. Rev. Lett.* **2004**, *92*, 048303-1–048303-4.
(53) Veniaminov, A.; Jahr, T.; Sillescu, H.; Bartsch, E. *Macromolecules* **2002**, *35*, 808–819.
(54) Thurau, C. T.; Ediger, M. D. *J. Chem. Phys.* **2003**, *118*, 1996–2004.
(55) Veniaminov, A.; Sillescu, H.; Bartsch, E. *J. Chem. Phys.* **2005**, *122*, 6.
(56) Schwille, P.; Korlach, J.; Webb, W. W. *Cytometry* **1999**, *36*, 176–182.
(57) Weiss, M.; Hashimoto, H.; Nilsson, T. *Biophys. J.* **2003**, *84*, 4043–4052.

(58) Fatin-Rouge, N.; Starchev, K.; Buffle, J. *Biophys. J.* **2004**, *86*, 2710–2719.
(59) Banks, D. S.; Fradin, C. *Biophys. J.* **2005**, *89*, 2960–2971.
(60) Wu, J. R.; Berland, K. M. *Biophys. J.* **2008**, *95*, 2049–2052.
(61) Saxton, M. J. *Biophys. J.* **1995**, *69*, 389–398.
(62) Saxton, M. J. *Biophys. J.* **1996**, *70*, 1250–1262.
(63) Wachsmuth, M.; Waldeck, W.; Langowski, J. *J. Mol. Biol.* **2000**, *298*, 677–689.
(64) Weiss, M.; Elsner, M.; Kartberg, F.; Nilsson, T. *Biophys. J.* **2004**, *87*, 3518–3524.
(65) Masuda, A.; Ushida, K.; Okamoto, T. *Phys. Rev. E* **2005**, *72*, 4.
(66) Rubinstein, M.; Colby, R. H. *Polymer Physics*; Oxford University Press: New York, 2003.